

Generalized predictive control of the aircraft system with actuator saturation to prevent Pilot-induced Oscillations

DOI:10.36909/jer.16725

P. Rezaei*, A. Khosravi**

, Faculty of Electrical and Computer Engineering, Babol Noshirvani University of
Technology, Babol, Mazandaran, Iran*

(*e-mail: pouya_rezaei2002@yahoo.com, **Corresponding Author e-mail: akhosravi@nit.ac.ir)

ABSTRACT

Amplitude and rate saturations are one of the problems of flight control systems which puts the closed-loop system stability at risk. These nonlinear elements are mainly responsible for the type II pilot induced oscillations (PIOs). In this paper, a robust unconstrained generalized predictive controller (GPC) with a self-tuning regulator (STR) structure is designed in the frequency domain to prevent the type II PIOs. Furthermore, the sensitivity function is used for tuning the GPC parameters and investigating the stability and robustness of the system against the uncertainties of the controller parameters. To get better results, a constrained GPC is further designed considering the rate, amplitude, and both saturations. Rate and amplitude saturations are considered as input constraints in the design stage. Finally, the performances of the proposed controllers are compared to that of a PID controller.

Keywords – Actuator Saturation; Flight Control System; Model Predictive Control; Pilot-induced Oscillations; Sensitivity Function.

INTRODUCTION

The actuator, one of the components of control loops of an aircraft, plays a prominent role in the flight system. However, the actuator saturations, that are amplitude and rate saturations existing in the real system as nonlinear elements, bring about some limitations for the aircraft (Welsch and Fichter, 2020, Yuan et al., 2020). Rate and amplitude saturations limit the system to execute commands and reject disturbances. Due to the saturation of the actuator, the output of the controller and the input of system may differ. Thus, the control action is no longer able to guide the system as its states cannot be properly updated, leading to system malfunction.

The pilot induced oscillations (PIOs) in modern flight control systems have deep roots in actuators' saturation (Bucolo et al., 2020). These oscillations are classified in type II of PIO, which is a quasi-linear oscillation with some nonlinear factors of the pilot-aircraft system (Jones, 2020). PIO is recognized as the instability in closed-loop system, including aircraft-pilot loop, which frequently occurs when the pilot is unable to adapt to the dynamics of the vehicle during high-performance flight operation. PIO occurs when there is 180 degrees of phase difference between aircraft's behavior or state, angular velocity, or normal acceleration and pilot's control inputs.

PIO is classified into three main categories:

- 1- Type I PIO: Linear oscillations of the pilot-aircraft system.
- 2- Type II PIO: quasi-linear oscillations with nonlinear elements of the pilot-aircraft system. The activation of rate or amplitude saturation is mainly responsible for this type of PIO.
- 3- Type III PIO: non-linear and unstable oscillations of the pilot-aircraft system.

Model Predictive Control (MPC) methods can be employed to tackle a wide diversity of control problems. In (Galuppini et al., 2018), the authors investigated actuator nonlinearities such as saturation and dead-zone in the control system and introduced two methods of Hybrid MPC and

standard MPC to solve this problem. In (Zaychik and Miller, 2019), the authors investigated the complex nonlinear behavior of a flight control system in a simulator of flight system at NASA Research Center. Introspective Control System (ICS) as a form of MPC is presented. In (Peng et al., 2017), a fast MPC with considering actuator saturation is designed for large-scale structures and compared with the standard MPC. In (Kassaeiyan et al., 2019) two methods of Linear MPC and Nonlinear MPC are designed to control the path tracking of the robotic system with considering the saturation range of the actuator. In (Song et al., 2016), an H_2/H_∞ distributed robust MPC is proposed for uncertain systems, and both actuator rate saturation and packet loss were considered. In these researches, different methods of MPC have been proposed to deal with saturation, but only some of them have precisely investigated the PIO phenomenon using MPC. In addition, the use of Generalized Predictive Control (GPC) has received less attention. The mentioned MPC methods do not investigate the uncertainty of MPC parameters. Furthermore, a specific method for tuning these parameters is not stated and most of them are based on trial and error. All of these points have been the impetus for this research.

This paper aims to propose a suitable generalized predictive controller to address the aforementioned problems. First, a robust unconstrained GPC with STR structure is proposed in the frequency domain. Then, to improve the results, the non-linear elements of actuator saturation are considered as input constraints, and the GPC is designed, first by considering the rate saturation and eventually with both rate and amplitude saturation. Finally, the designed controllers are compared to the PID controller.

MATHEMATICAL MODEL OF THE SYSTEM

In (Wenqian et al., 2010) a model for the flight nominal conditions of T-33 jet is presented.

$$G(s) = \frac{q(s)}{\delta_e(s)} = \frac{(\tau s + 1)\omega_s^2}{s(s^2 + 2\xi_s\omega_s s + \omega_s^2)} \quad (1)$$

in which $\tau = 0.8$ s, $\omega_s = 4.9$ rad/s, $\zeta_s = 0.7$, q and δ_e are the pitch rate and the deflection of elevator.

The control block is depicted in Figure 1. As one can see, it includes the rate and amplitude limit saturation, in which u'' is the control input to the actuator and $\omega_a = 20.2$ (rad/s) is the cutoff frequency. Upper and lower rate limits occur at 10 deg/s and -10 deg/s, respectively. Moreover, the upper and lower amplitude saturation limits occur at 10 deg and -10 deg, respectively.

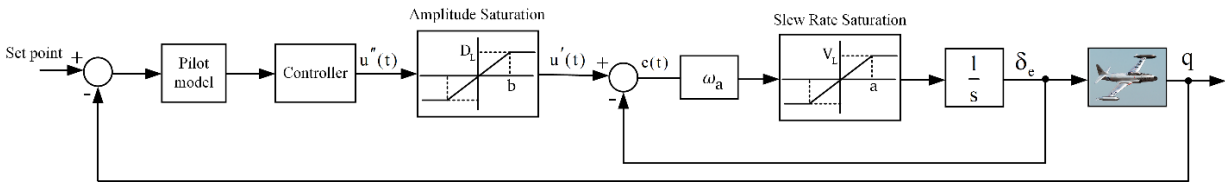


Figure1. Control block diagram.

GENERALIZED PREDICTIVE CONTROL

The GPC was designed by Clark et al. (Clarke et al., 1987), and it has turned into one of the well-known and favorite methods of predictive control in industry and research. This method can be used to control an unstable and non-minimum phase systems.

This paper uses the CARIMA model (Eq. 2), which is the basis for GPC:

$$A(z^{-1})y(t)\Delta = z^{-d}B(z^{-1})\Delta u(t-1) + T(z^{-1})e(t) \quad (2)$$

$$A(z^{-1}) = 1 + a_1z^{-1} + a_2z^{-2} + \dots + a_{n_a}z^{-n_a}$$

$$B(z^{-1}) = b_0 + b_1z^{-1} + b_2z^{-2} + \dots + b_{n_b}z^{-n_b}$$

$$T(z^{-1}) = 1 + t_1z^{-1} + t_2z^{-2} + \dots + t_{n_t}z^{-n_t}$$

$$\Delta = 1 - z^{-1}$$

where, $y(t)$, $u(t)$, and d represent the system output and input and delay time, respectively. $e(t)$ denotes the white noise with zero mean, and A , B , and T are polynomials of backward shift actuator.

The following cost function:

$$J(N_1, N_2, N_u) = \sum_{j=1}^{N_u} r(j) [\Delta u(t+j-1)]^2 + \sum_{j=N_1}^{N_2} q(j) [\hat{y}(t+j|t) - y_d(t+j)]^2 \quad (3)$$

should be minimized, $\hat{y}(t+j|t)$ is j step ahead prediction of the plant output. N_1 , N_2 , and N_u are the minimum prediction horizon, maximum prediction horizon, and the control horizon. $q(j)$ and $r(j)$ are the weighting sequences; defined as follows:

$$\begin{aligned} q(i) &= \beta^{-2i} & i &= N_1, N_1 + 1, \dots, N_2 \\ r(j) &= \rho \beta^{-2j} & j &= 1, 2, \dots, N_u \end{aligned} \quad (4)$$

$y_d(t+j)$ is the future reference trajectory obtained by filtering the ideal reference trajectory $r(t+j)$.

1. GPC with STR Structure

Now, it is turn to design a GPC controller with an STR structure (Camacho and Alba, 2013), its closed-loop relations must be converted to a block diagram of Figure 2, where R and S are polynomials.

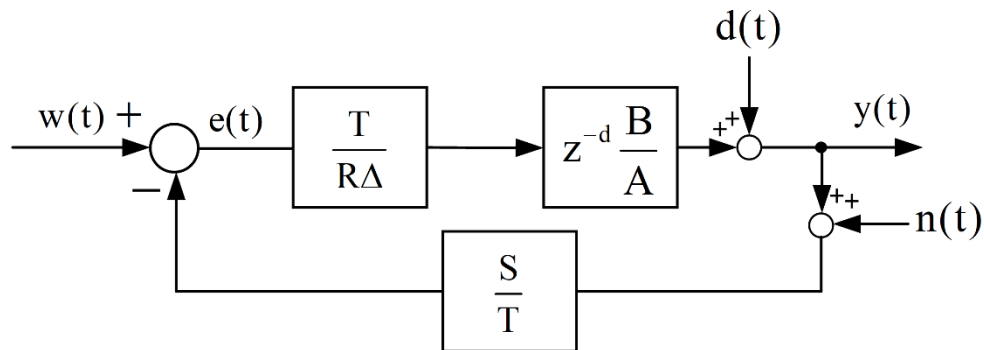


Figure 2. The GPC with the STR structure with noise and disturbance.

After some manipulations, one can end up with the following control rule:

$$\Delta u(t) = \frac{T(z^{-1})}{R(z^{-1})} w(t) - \frac{S(z^{-1})}{R(z^{-1})} y(t) \quad (5)$$

To find the optimal value of the cost function in (3), we use the Diophantine equation in (6) to optimally predict $\hat{y}(t+j)$, as follows:

$$\begin{aligned} T(z^{-1}) &= A(z^{-1})E_j(z^{-1})\Delta + F_j(z^{-1})z^{-j} \\ N_1 \leq j &\leq N_2 \end{aligned} \quad (6)$$

Another Diophantine equation is defined as follows:

$$E_j(z^{-1})B(z^{-1}) = T(z^{-1})H_j(z^{-1}) + I_j(z^{-1})z^{-j} \quad (7)$$

If $T(z^{-1}) = 1$, then the best predictions for future outputs are as follows:

$$\hat{y}(t+j) = \Delta u(t+j)H_j(z^{-1}) + f(t+j) \quad (8)$$

where f is the system's free response, as follows:

$$f(t+j) = I_j(z^{-1})\Delta u(t-1) + F_j(z^{-1})y(t) \quad (9)$$

Future control signals are obtained as follows:

$$\Delta U = (G^T Q G + R)^{-1} G^T Q (Y_d - f) = K(Y_d - f) \quad (10)$$

The first control signal is obtained using the first row of the K :

$$\Delta u(t) = K_1 (Y_d - f) = \sum_{j=N_1}^{N_2} k_j \left[w(t+j) - \frac{F_j(z^{-1})}{T(z^{-1})} y(t) - \frac{I_j(z^{-1})}{T(z^{-1})} \Delta u(t) z^{-1} \right] \quad (11)$$

$S(q^{-1})$ and $R(q^{-1})$ polynomials are obtained by comparing Eqs. (11) and (5) as follows:

$$R(z^{-1}) = \frac{T(z^{-1}) + z^{-1} \sum_{i=N_1}^{i=N_2} k_i I_i}{\sum_{i=N_1}^{i=N_2} k_i}, \quad S(z^{-1}) = \frac{\sum_{i=N_1}^{i=N_2} k_i F_i}{\sum_{i=N_1}^{i=N_2} k_i} \quad (12)$$

$y(t)$ is obtained by replacing the calculated control signal in the closed-loop relation, as follows:

$$y(t) = \frac{BTz^{-1}}{RA\Delta + BSz^{-1}} w(t) + \frac{TR}{RA\Delta + BSz^{-1}} e(t) \quad (13)$$

2. Robustness Analysis of GPC

When it comes to control engineering, it is of crucial importance to address the stability issues of the control system as well as its robustness to system uncertainties (Naeijian and Khosravi, 2020, Bijani and Khosravi, 2018). In this section, the sensitivity function is used for tuning the GPC parameters and investigating the robustness and stability of the system against the uncertainties of the controller parameters. It worths mentioning that for the phase margin and gain margin greater or equal to 29 degrees and 6 dB, respectively, and a delay margin equal to the sampling time ($\Delta\tau = T_s$), the system has good robustness while its stability is guaranteed (Landau, 1998). Therefore, using the sensitivity functions, the bounds are designed in such a way that these cases are established.

Assuming that the noise and turbulence of the output are entered in the control loop as Figure 2, one can write the closed-loop equations as follows:

$$y(t) = \frac{BTz^{-1}}{RA\Delta + BSz^{-1}} w(t) + \frac{AR\Delta}{RA\Delta + BSz^{-1}} d(t) - \frac{BSz^{-1}}{RA\Delta + BSz^{-1}} n(t) \quad (14)$$

where $d(t)$ is the output disturbance and $n(t)$ is the output noise. The transfer function of $d(t)$ to $y(t)$, which is the transfer function of output sensitivity to output disturbance, is defined as follows:

$$S_{y_d}(z^{-1}) = \frac{AR\Delta}{RA\Delta + BSz^{-1}} \quad (15)$$

The transfer function of $n(t)$ to $y(t)$ is the sensitivity of the system output to noise:

$$S_{y_n}(z^{-1}) = \frac{-BSz^{-1}}{RA\Delta + BSz^{-1}} \quad (16)$$

To form the robust bounds, a concept called *modulus margin*, or ΔM is used which is obtained by the minimum distance between the open-loop transfer function $G(z^{-1})$ and the point $(-1, 0)$.

$$\Delta M = |1 + G_{OL}|_{\min} = \left| \frac{RA\Delta + BSz^{-1}}{AR\Delta} \right|_{\min} = \left(\|S_{y_d}(z^{-1})\|_{\max} \right)^{-1} = \left(\|S_{y_d}(z^{-1})\|_{\infty} \right)^{-1} \quad (17)$$

The following relations exist between ΔM , phase margin ($\Delta\phi$), and gain margin, (ΔG):

$$\Delta G \geq \frac{1}{1 - \Delta M}, \quad \Delta\phi = 2 \arcsin\left(\frac{\Delta M}{2}\right) \geq \Delta M \quad (18)$$

Given the above equations, the value of ΔM must be greater than or equal to 0.5 to have the desired value of gain and phase margins.

There is another concept that shows the consistency of the system in the face of uncertainty in delay, which is called *delay margin*.

The delay margin, or $\Delta\tau$ is equal to the maximum amount of delay that can be added to a open-loop system while system can remain stable. The following equation exists for the delay margin:

$$\Delta\tau = \frac{\Delta\phi}{\omega_{cr}} \quad (19)$$

where $\Delta\phi$ is the phase margin and ω_{cr} is the crossover frequency.

Let us consider two systems $G_1 = \frac{B}{A}$ and $G_2 = \frac{Bz^{-1}}{A}$ with a unit delay. As a unit delay is

desirable for the system, the following relations are established between the two systems:

$$|G_{2OL} - G_{1OL}| < |1 + G_{1OL}| \quad (20)$$

By replacing G_1 and G_2 we will have:

$$\left| \frac{Bz^{-1}}{A} - \frac{B}{A} \right| < |S_{y_d}^{-1}| \quad (21)$$

$$\frac{\left| \frac{Bz^{-1}}{A} - \frac{B}{A} \right|}{\left| \frac{B}{A} \right|} < |S_{y_n}^{-1}| \quad (22)$$

And as a result, using the equation $S_{y_d}(z^{-1}) - S_{y_n}(z^{-1}) = 1$, one can conclude that:

$$1 + \frac{1}{|1 + z^{-1}|} < |S_{y_d}| < 1 + \frac{1}{|1 - z^{-1}|} \quad (23)$$

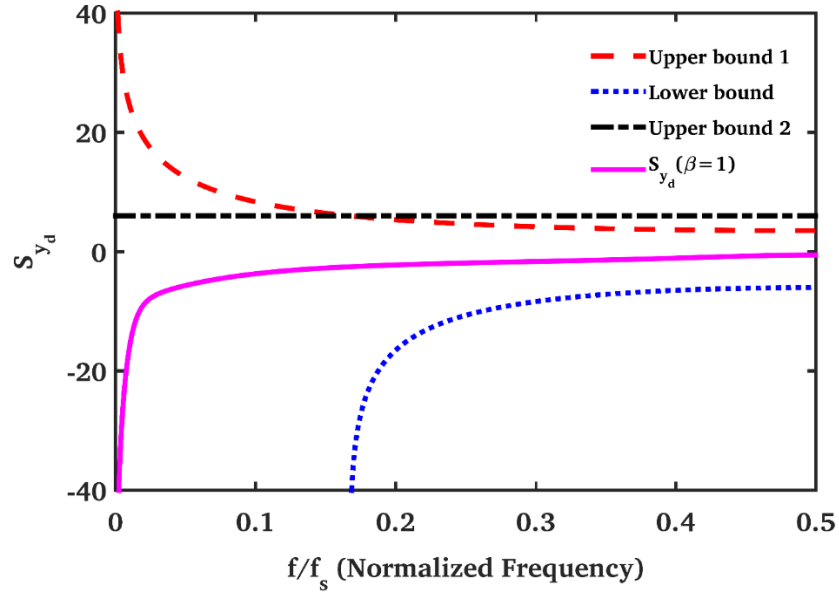
So considering (23) and:

$$\|S_{y_d}(z^{-1})\|_{\infty} < 2 \quad (24)$$

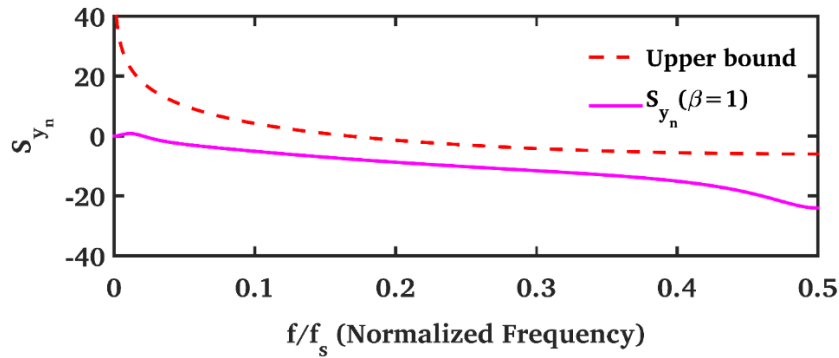
the GPC parameters must be selected so that $S_{y_d}(z^{-1})$ and $S_{y_n}(z^{-1})$ can remain within the above bounds. It is obvious from Figure 3 that for the parameters in Table 1, $S_{y_d}(z^{-1})$ and $S_{y_n}(z^{-1})$ are placed inside the robust bounds, and the system has good robustness.

Table 1. Simulation Parameters

Parameter	Value
α	0.5
N_1	1
N_2	20
N_u	10



(a) Output sensitivity function to disturbance bounds.



(b) Output sensitivity function to noise bounds.

Figure 3. Robust bounds for $\beta = 1$.

CONSTRAINED GPC WITH RATE SATURATION

Considering the rate saturation, the control signal (continuous-time) must be in the following range:

$$\dot{u}_{\min} \leq \dot{u} \leq \dot{u}_{\max} \quad (25)$$

where $\dot{u}_{\max} = 10^\circ / s$ and $\dot{u}_{\min} = -10^\circ / s$. In discrete time, one can write:

$$\Delta \mathbf{u}_{\min} \leq \Delta \mathbf{u} \leq \Delta \mathbf{u}_{\max} \quad (26)$$

where:

$$\Delta \mathbf{u}_{\max} = \dot{\mathbf{u}}_{\max} \mathbf{T}_s, \Delta \mathbf{u}_{\min} = \dot{\mathbf{u}}_{\min} \mathbf{T}_s \quad (27)$$

One can re-write (26) as follows:

$$\begin{bmatrix} \mathbf{I}_{N_u} \\ -\mathbf{I}_{N_u} \end{bmatrix} \Delta \mathbf{U}(t) \leq \begin{bmatrix} \Delta \mathbf{U}_{\max} \\ -\Delta \mathbf{U}_{\min} \end{bmatrix} \quad (28)$$

where $\Delta \mathbf{U}(t)$ includes the increments in future control signals as follows:

$$\Delta \mathbf{U}(t) = \begin{bmatrix} \Delta \mathbf{u}(t) \\ \Delta \mathbf{u}(t+1) \\ \Delta \mathbf{u}(t+2) \\ \vdots \\ \Delta \mathbf{u}(t+N_u-1) \end{bmatrix} \quad (29)$$

Also, $\Delta \mathbf{U}_{\max}$ and $\Delta \mathbf{U}_{\min}$ are the vectors with N_u entries.

CONSTRAINED GPC WITH RATE AND AMPLITUDE SATURATION

Now, considering the amplitude saturation, the control signal (continuous-time) must be in the following range:

$$\begin{aligned} \mathbf{u}_{\min} &\leq \mathbf{u}(t) \leq \mathbf{u}_{\max} \\ \mathbf{u}_{\min} &\leq \mathbf{u}(t+1) \leq \mathbf{u}_{\max} \\ &\vdots \\ \mathbf{u}_{\min} &\leq \mathbf{u}(t+N_u-1) \leq \mathbf{u}_{\max} \end{aligned} \quad (30)$$

Therefore, the constraints on the amplitude can be formulated as:

$$\begin{aligned} \bar{S}\Delta U + U^- &\leq U_{\max} \\ -(\bar{S}\Delta U + U^-) &\leq -U_{\min} \end{aligned} \quad (31)$$

which can be written as follows:

$$\begin{bmatrix} \bar{S} \\ -\bar{S} \end{bmatrix} \Delta U(t) \leq \begin{bmatrix} U_{\max} - U^- \\ -(U_{\min} - U^-) \end{bmatrix} \quad (32)$$

where U_{\max} and U_{\min} are vectors with N_u entries.

The cost function is as follows:

$$J = (\Delta UG + f - Y_d)^T Q(\Delta UG + f - Y_d) + \Delta U^T R \Delta U \quad (33)$$

We can convert the above cost function into standard quadratic programming (QP):

$$J = \frac{1}{2} \Delta U(t)^T H \Delta U(t) + c^T \Delta U(t) + c_0 \quad (34)$$

where by defining $Y_d - f \square E$, H , c , and c_0 are as follows:

$$H = 2(G^T QG + R), \quad c = -2G^T QE, \quad c_0 = E^T QE \quad (35)$$

At any sampling time, the cost function (34) should be solved considering constraints (28) and (32). This is done by using the QP method in MATLAB environment.

SIMULATION RESULTS

In this section, the simulations of all three GPCs as well as a PID controller are shown and compared with each other to show the accuracy of the design. The PID controller is designed by classical methods using gain and phase margin. The performances of the above controllers are shown in Figure 4. It is obvious that the output tracking is better performed in the GPCs as compared to PID controller. It can also be seen that the constrained GPC with the amplitude and rate saturation outperforms other controllers in terms of reference tracking.

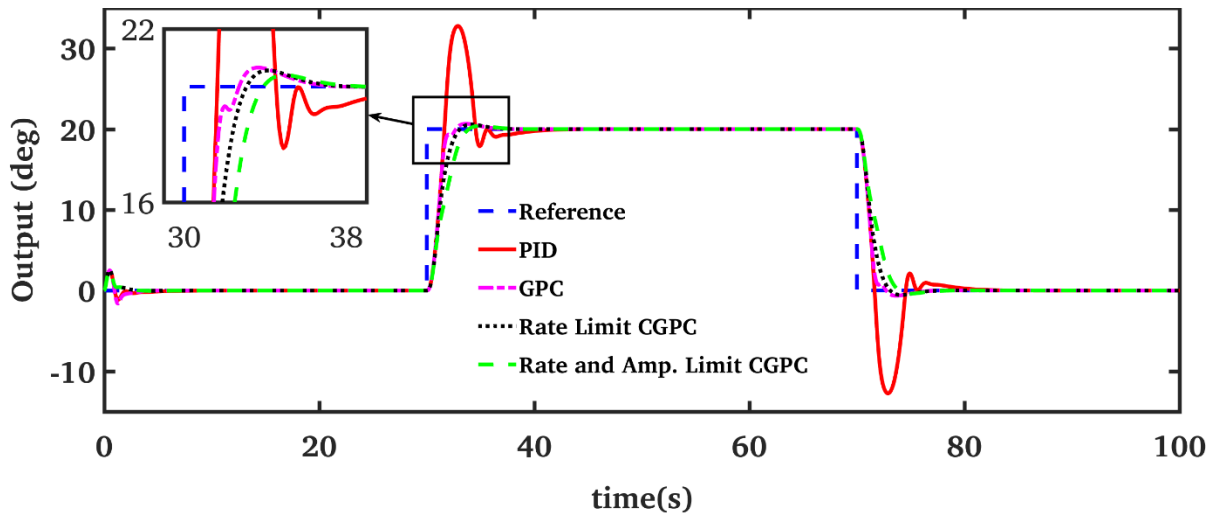


Figure 4. The output responses of the robust unconstrained GPC, CGPC, and PID.

The control signals of the above controllers are shown in Figure 5, where one can see that the value of the control signal in the CGPC Rate Limit controller does not exceed ± 8 degrees. In both Rate Limit CGPC and Rate and Amp. Limit CGPC, the control commands are issued at all times so that the rate does not exceed the designer's desired value (which is constrained at $10^\circ / s$ here). In this figure, again, the constrained GPC has shown more favorable behavior by considering the saturation of the rate and amplitude.

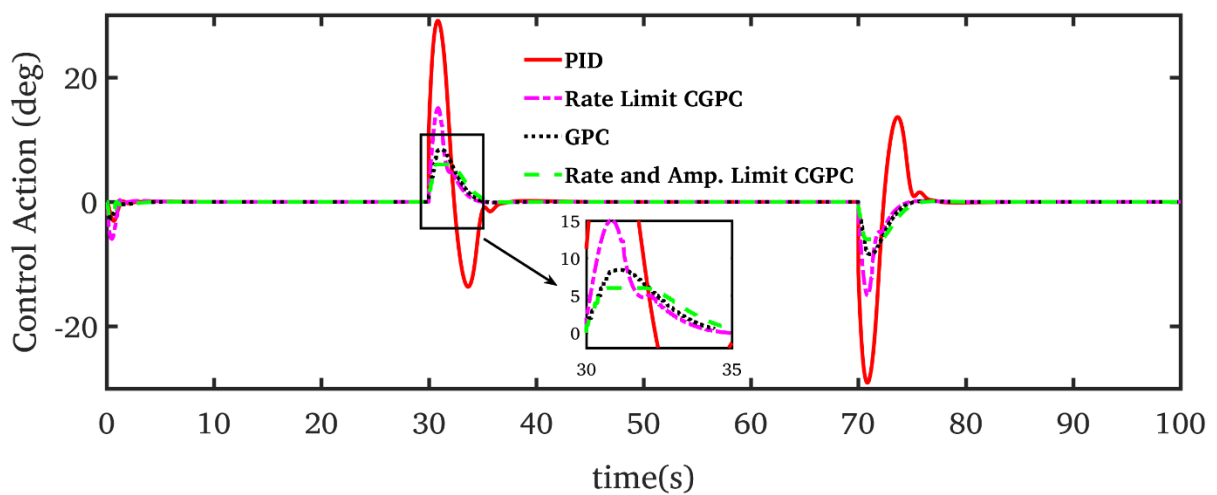


Figure 5. The control action of the robust unconstrained GPC, CGPC, and PID.

As Figure 5 shows, the rate and amplitude limit GPC performs better than other controllers because it penalizes both the rate and amplitude of the control action. Also, the rate of the control signal is shown in Figure 6 that constrained GPC has less control effort.

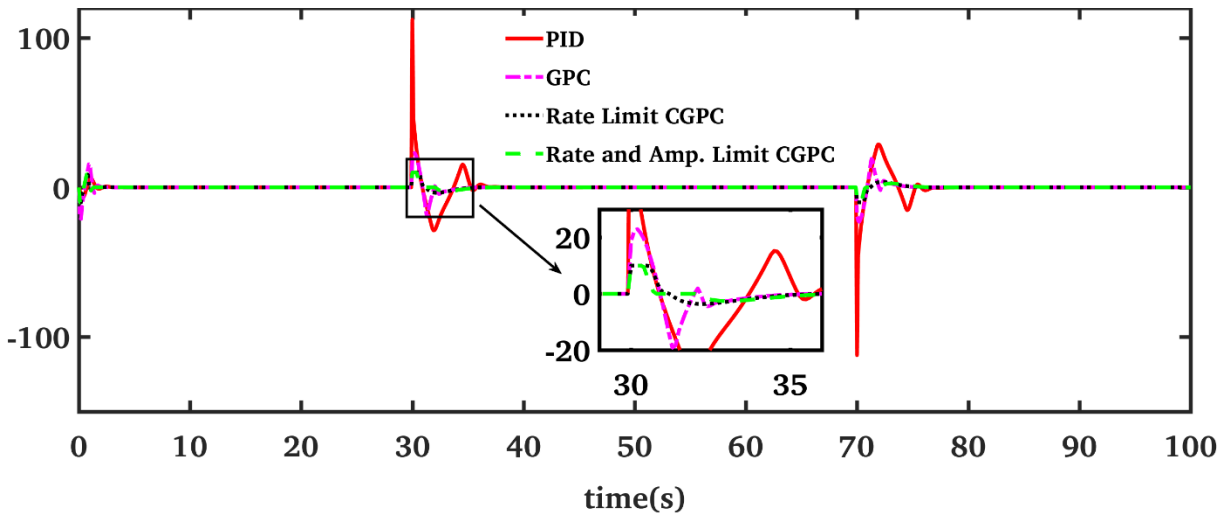


Figure 6. The rate of control action of the robust unconstrained GPC, CGPC, and PID.

According to Figure 6, the performance of constrained GPCs is better than other controllers.

CONCLUSION

In this paper, a robust unconstrained GPC was proposed. It used a STR structure to prevent the type II PIOs resulted from actuators' rate and amplitude saturation. Furthermore, the tuning of GPC weights and parameters is done in the frequency domain using the robust control approach. A constrained GPC including the rate, amplitude, or both saturation types as input constraints in the design stage was also designed. The results showed that the constrained GPC that considers the rate and amplitude saturation provided a far better performance as compared to other controllers.

REFERENCES

- BIJANI, V. & KHOSRAVI, A. 2018.** Robust PID controller design based on H_∞ theory and a novel constrained artificial bee colony algorithm. *Transactions of the Institute of Measurement and Control*, 40, 202-209.
- BUCOLO, M., BUSCARINO, A., FORTUNA, L. & GAGLIANO, S. 2020.** Bifurcation scenarios for pilot induced oscillations. *Aerospace Science and Technology*, 106, 106194.
- CAMACHO, E. F. & ALBA, C. B. 2013.** *Model predictive control*, Springer science & business media.
- CLARKE, D. W., MOHTADI, C. & TUFFS, P. 1987.** Generalized predictive control—Part I. The basic algorithm. *Automatica*, 23, 137-148.
- GALUPPINI, G., MAGNI, L. & RAIMONDO, D. M. 2018.** Model predictive control of systems with deadzone and saturation. *Control Engineering Practice*, 78, 56-64.
- JONES, M. 2020.** The use of the Open-Loop Onset Point (OLOP) to predict rotorcraft pilot-induced oscillations. *CEAS Aeronautical Journal*, 11, 693-711.
- KASSAEIYAN, P., TARVIRDIZADEH, B. & ALIPOUR, K. 2019.** Control of tractor-trailer wheeled robots considering self-collision effect and actuator saturation limitations. *Mechanical Systems and Signal Processing*, 127, 388-411.
- LANDAU, I. 1998.** The RST digital controller design and applications. *Control Engineering Practice*, 6, 155-165.
- NAEIJIAN, M. & KHOSRAVI, A.** Stability Analysis of Model Reference Adaptive Control with the New Theorem of Stability. 2020 28th Iranian Conference on Electrical Engineering (ICEE), 2020. IEEE, 1-6.
- PENG, H., LI, F., ZHANG, S. & CHEN, B. 2017.** A novel fast model predictive control with actuator saturation for large-scale structures. *Computers & Structures*, 187, 35-49.
- SONG, Y., FANG, X. & DIAO, Q. 2016.** Mixed H_2/H_∞ distributed robust model predictive control for polytopic uncertain systems subject to actuator saturation and missing measurements. *International Journal of Systems Science*, 47, 777-790.
- WELSCH, M. & FICHTER, W.** Control of Large Multicopters with Rate-Limited Electric Motors. AIAA Scitech 2020 Forum, 2020. 1832.
- WENQIAN, T., EFREMOV, A. & XIANGJU, Q. 2010.** A criterion based on closed-loop pilot-aircraft systems for predicting flying qualities. *Chinese Journal of Aeronautics*, 23, 511-517.
- YUAN, J., FEI, S. & CHEN, Y. 2020.** Compensation strategies based on Bode step concept for actuator rate limit effect on first-order plus time-delay systems. *Nonlinear Dynamics*, 1-16.
- ZAYCHIK, K. & MILLER, T.** Introspective Control Systems: Fast Model Predictive Control with Explicit Optimization Search, Nonlinear Models, and On-line Learning. AIAA Scitech 2019 Forum, 2019. 0424.